Electrochemistry Communications 90 (2018) 106–110

Contents lists available at ScienceDirect

Electrochemistry Communications

journal homepage: www.elsevier.com/locate/elecom

Selective electro-oxidation of glycerol over Pd and Pt@Pd nanocubes

Yongfang Zhou, Yi Shen*

School of Food Science and Engineering, South China University of Technology, Guangzhou 510640, China

ARTICLE INFO

Keywords:
Pd nanocubes
Core-shell structure
Glycerol electro-oxidation
Selectivity
Facet-dependent activity

ABSTRACT

Well-defined Pd and Pt encapsulated Pd (Pt@Pd) nanocubes (NCs) are examined as catalysts for the electro-oxidation of glycerol in alkaline solutions. Pt@Pd shows the highest current density of 3.22 mA cm^{-2}, which is 3.5, 4.8 and 1.5 times those of Pd/C, Pt/C and Pd NCs. Pd NCs possess the largest glyceraldehyde selectivity of 61.2% while Pt@Pd facilitates the yield of glycolic acid.

1. Introduction

Being an abundant biomass, glycerol (GLY) can be converted into many value-added chemicals and intermediates, such as dihydroxyacetone, glyceraldehyde (GALD), glycolic acid (GA), tartronic acid (TA), and glyceric acid (GLA) via heterogeneous catalytic and enzymatic processes [1–6]. Among the various approaches, electrochemical oxidation affords a totally green route to produce valuable chemicals from GLY. GLY electro-oxidation is a very complex process, which involves many intermediates and products [7–10]. Developing electrocatalysts with high activity and selectivity holds the key to the feasibility of this process. To date, numerous studies have been devoted to exploring catalysts while limited work has focused on the mechanism and pathways of GLY oxidation [11–24]. Herein, Pd nanocubes (NCs) and Pt encapsulated Pd (Pt@Pd) nanoparticles (NPs) are examined as catalysts for the electro-oxidation of glycerol in alkaline solutions. The activity of the resulting Pd NCs and Pt@Pd NPs are studied by cyclic voltammetry and benchmarked against those of commercial Pd/C and Pt/C catalysts. The products of GLY oxidation over the catalysts at three applied potentials (i.e., −0.4, −0.1 and 0.2 V) were analyzed by high-performance liquid chromatography (HPLC). On the basis of HPLC results, the reaction pathways of GLY oxidation were proposed.

2. Experimental

2.1. Synthesis and characterization of catalysts

Pd NCs were prepared according to the method reported by Jin et al. [25,26]. The resulting product was dispersed into 5 mL of water for further use. Pt@Pd NPs were synthesized via a seed-mediated growth method. First, 20 mL of 100 mM CTAB, 10 mL of 10 mM KI solution and 400 uL of the as-synthesized Pd NCs were thoroughly mixed and preheated at 90 °C for 10 min to form a stable suspension. Next, 500 uL of 10 mM H_2PtCl_6 was added. Subsequently, 600 uL of freshly prepared 100 mM ascorbic acid was introduced into the mixture. The reaction was conducted at 90 °C for 3 h. The product was separated by centrifugation, thoroughly washed, and re-dispersed in deionized water. The morphology of the catalysts was observed by transmission electron microscopy (TEM, JEOL JEM-2010, Japan). An Energy dispersive X-ray spectroscopy (EDX) analyzer equipped in the TEM was used to analyze the elemental composition of the samples.

2.2. Electrochemical measurements

The electrochemical activity of the catalysts was evaluated by a typical three-electrode cell connected with a potentiostat (CHI 660E). The details of experimental procedures are described in the authors' previous work [27–30]. The catalyst loading in the working electrode is ca. 180 μg cm^{-2}. For product analysis, an H-type cell with two compartments separated by an anionic membrane was used. The volume of the electrolyte in each chamber was 20 mL. A graphite paper (10 mm × 10 mm) was used as a working electrode. A saturated calomel electrode (SCE) and Pt gauze were used as reference and counter electrodes, respectively. Before experiments, all the electrolytes were purged with nitrogen for 30 min. All the potentials in this work were referenced to the SCE. The electrochemical measurements were conducted at ambient temperature.

2.3. Product analysis

The products of GLY oxidation were analyzed by HPLC (Agilent 1260 Infinity) equipped with a refractive index detector and a multiple

* Corresponding author.
E-mail address: feyshen@scut.edu.cn (Y. Shen).

https://doi.org/10.1016/j.elecom.2018.04.012
Received 28 March 2018; Received in revised form 6 April 2018; Accepted 11 April 2018
Available online 13 April 2018
1388-2481/

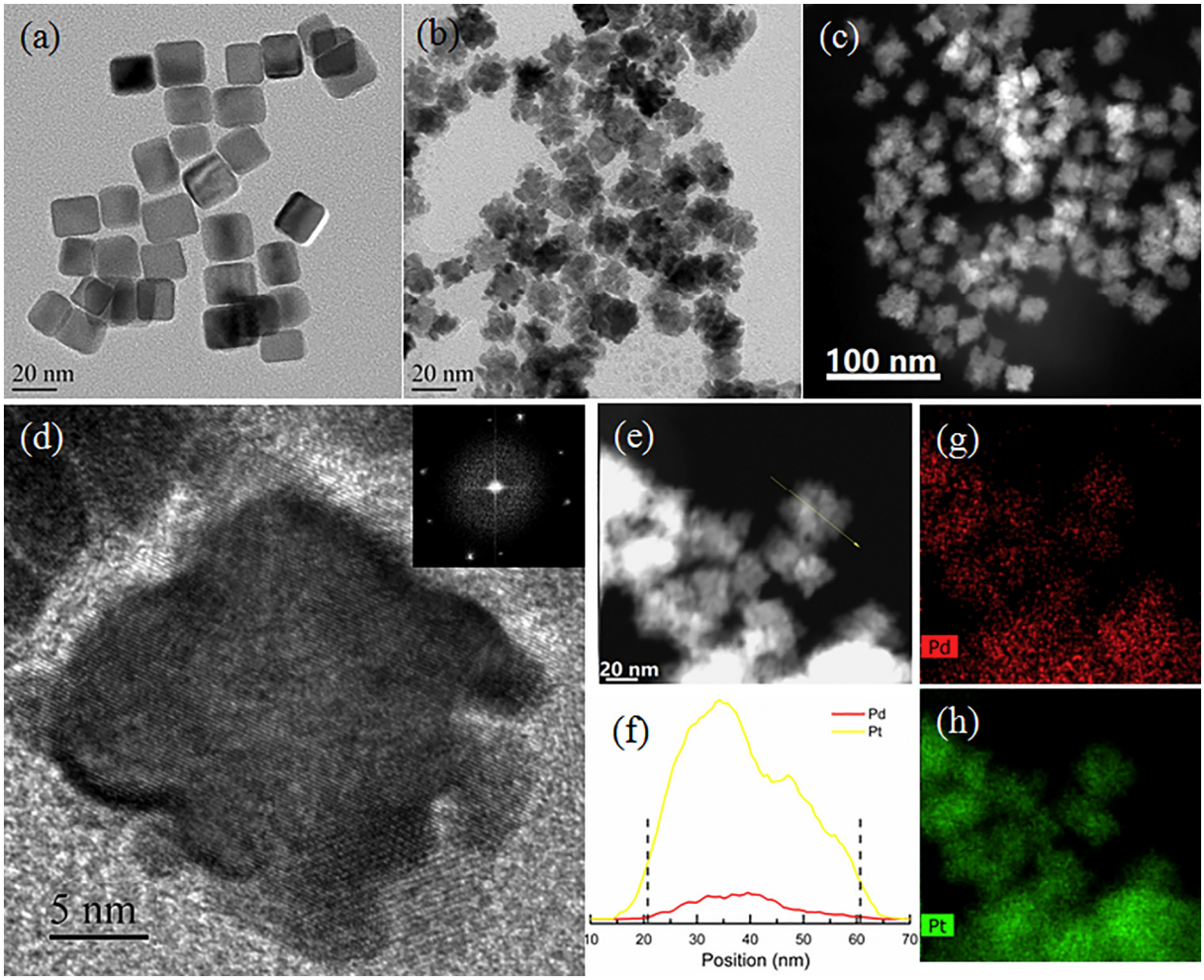

Fig. 1. (a) and (b) TEM images of Pd NCs and Pt@Pd NPs, respectively. (c) HAADF-TEM image, (d) HRTEM image, (e) HAADF-TEM image, (f) line scan profile, and (g, h) EELS elemental mapping micrographs of Pt@Pd NPs.

wavelength detector. An Aminex HPX-87H (Bio-Rad) column was used for product separation. The eluent was 5 mM H_2SO_4 with a flow rate of 0.5 mL min^{-1} and the temperature of the column was kept at 65 °C. Chronoamperometry measurements were conducted for 2 h under applied potentials of −0.4, −0.1 and 0.2 V. Subsequently, the electrolyte solution was collected with a syringe for HPLC analysis. The selectivity (S_i) of each product was calculated by following equation: $S_i = c_i/\Sigma\, c_i$, where c_i is the concentration of product *i*.

3. Results and discussion

3.1. Structural properties

The morphology of the as-prepared catalysts was studied by TEM. Fig. 1a shows the TEM image of the Pd NCs. The resulting uniform Pd NCs possess an average edge length of ca. 22 ± 2.6 nm. A representative TEM image of Pt@Pd NPs (shown in Fig. 1b) clearly reveals the presence of uneven Pt layers surrounding Pd NCs, leading to rather rough surface. The deposition of Pt on Pd NC seeds is also noted from high-angle annular dark-field scanning TEM image (shown in Fig. 1c). There is clear contrast between the Pt shell and Pd core because of the difference in atomic number between these two elements. The core-shell structure of Pt@Pd NPs is verified by high-resolution TEM (HRTEM) as shown in Fig. 1d. It clearly shows that the lattice fringes are coherently extended from the Pd core to Pt shell, indicating an epitaxial growth of Pt on Pd NCs [31]. Notably, some voids are present in the nanoparticles, which could be related to the fast kinetics of the galvanic process [32]. The inset shown in Fig. 1d displays the selected area electron diffraction of the Pt@Pd NP which consists of two sets of diffraction patterns, corresponding to the Pd core and Pt shell, respectively. The HAADF-STEM micrograph (shown in Fig. 1e) and corresponding electron energy-loss spectroscopy (EELS) elemental mapping micrographs (shown in Fig. 1g, h) vividly resolved the distribution of Pt and Pd. The line scan result shown in Fig. 1f further confirmed the core-shell structure of Pt@Pd NPs. A close examination on the distribution profiles could reveal that the thickness of the Pt shell is around 5 nm.

3.2. Electrochemical activity

Because the hydrogen adsorption-desorption in Pd/Pt crystals are highly sensitive to the surface structure, the corresponding voltammograms in 1 M KOH were first recorded (the insets in Fig. 2) and utilized as fingerprints to probe valuable information such as densities of crystal facets. The commercial Pd/C (10 wt%) and Pt/C (40 wt%) catalysts consist of metal NPs with diameters less than 5 nm supported by carbons. The voltammograms of the Pd/C (see the inset in Fig. 2a) and Pt/C catalysts (see the inset in Fig. 2b) are characteristic of polyoriented metal NPs. The voltammograms of Pt/C and Pd/C show thicker double layer zones, which is attributed to the capacitive properties of the carbon supports in the catalysts. Comparing with the Pd/C catalyst, the as-synthesized Pd NCs show well-defined peaks associated with